

# High-dimensional Outlier Detection via Stability

Qiang Heng\*, Hui Shen<sup>†</sup>, Kenneth Lange<sup>‡</sup>

## Abstract

The Minimum Covariance Determinant (MCD) method is a widely adopted tool for robust estimation and outlier detection. In this paper, we introduce a new framework for model selection in MCD with spectral embedding based on the notion of stability. Our best subset algorithm leverages principal component analysis for dimension reduction, statistical depths for effective initialization, and concentration steps for subset refinement. Subsequently, we construct a bootstrap procedure to estimate the instability of the best subset algorithm. The parameter combination exhibiting minimal instability proves ideal for the purposes of high-dimensional outlier detection, while the instability path offers insights into the inlier/outlier structure. We rigorously benchmark the proposed framework against existing MCD variants and illustrate its practical utility on two spectra data sets and a cancer genomics data set.

*Keywords:* Outlier detection; Principal component analysis; Statistical depth; Bootstrap; Stability; Model selection; Exploratory data analysis

## 1 Introduction

The minimum covariance determinant (MCD) estimator ([Rousseeuw, 1985](#)) and its subsequent extensions have been widely adopted for robust estimation of multivariate location and scatter and outlier detection. This estimator identifies a subset of a predetermined size from an  $n \times p$  multivariate data matrix, aiming for the smallest possible determinant of the reduced sample covariance matrix. MCD rose in popularity after the introduction of the computationally efficient fast minimum covariance determinant (FastMCD)

---

\*Department of Computational Medicine, UCLA

<sup>†</sup>Department of Mathematics and Statistics, McGill University

<sup>‡</sup>Departments of Computational Medicine, Human Genetics, and Statistics, UCLA

algorithm (Rousseeuw and Driessen, 1999). FastMCD has found broad applications in finance, econometrics, engineering, the physical sciences, and biomedical research (Hubert et al., 2008, 2018). The minimum covariance determinant estimator is statistically consistent and asymptotically normal (Butler et al., 1993; Cator and Lopuhaä, 2012). Recent extensions to the MCD paradigm include a kernelized version (Schreurs et al., 2021) for nonelliptical data and a cell-wise version (Raymaekers and Rousseeuw, 2023) for robustness against cell-wise outliers.

In the univariate case (Rousseeuw and Leroy, 2005), the MCD problem can be exactly solved in  $O(n \log n)$  arithmetic operations. Unfortunately, computation becomes much more challenging in the multivariate setting. FastMCD is essentially a greedy block minimization algorithm, providing a locally optimal solution for the nonconvex, combinatorial optimization problem of minimizing the subsample covariance determinant. Given its greedy nature, FastMCD can be trapped by local minima. Therefore, proper initialization is crucial, particularly as the proportion of outliers or the dimensionality of the data grows. Naive random initialization falters in these circumstances. Hubert et al. (2012) propose a deterministic initialization strategy called deterministic minimum covariance determinant (DetMCD) that relies on six different initializations for  $\mu$  and  $\Sigma$ . This ensemble strategy can greatly outperform random initialization in robustness and speed when the proportion of outliers is high. However, recent work by Zhang et al. (2023) demonstrates that using the trimmed subset induced by the notion of projection depth (Zuo and Serfling, 2000a) is conceptually simpler, computationally faster, and even more robust. This is likely due to the fact that asymptotically, projection depth and MCD induces the same elliptical decision region (Zuo and Serfling, 2000b).

To its detriment, MCD relies on the computation of Mahalanobis distances, which requires the invertibility of  $\hat{\Sigma}$ . To tackle the high-dimensional scenario  $p > n$ , Boudt et al. (2020) add Tikhonov regularization to the covariance matrix to ensure its positive definiteness. However, their minimum regularized covariance determinant (MRCD) estimator is computationally expensive due to its need to invert large matrices at each iteration. Other tactics for high-dimensional outlier detection rely on alternative definitions of Mahalanobis distance and formulate the problem in the framework of hypothesis testing. For example, Ro et al. (2015), Li and Jin (2022), and Li et al. (2024) study the null asymptotic distribution in this context under suitable model assumptions.

This paper illustrates a new workflow for high-dimensional outlier detection founded

on the concept of stability. We first propose a best subset selection algorithm that integrates spectral embedding, statistical depth, and concentration steps. The use of principal components for dimension reduction in outlier detection was previously explored by [Hubert et al. \(2005\)](#) and [Filzmoser et al. \(2008\)](#). Compared with these existing approaches, our algorithm does not require a robust estimate of covariance matrices. We demonstrate that ordinary PCA is sufficient for revealing inlier/outlier structure and that outlier detection can be performed after spectral embedding. We then construct a bootstrap procedure for simultaneously estimating the number of inliers  $h$  and the appropriate number of principal components  $q$ .

The current literature largely ignores principled ways of selecting  $h$ . Often  $h$  is chosen conservatively to ensure the exclusion of every conceivable outlier from the selected subset. Popular choices include  $h = \lfloor 0.5n \rfloor$  and  $h = \lfloor 0.75n \rfloor$ . These arbitrary choices potentially compromise statistical efficiency. Although various reweighting procedures ([Rousseeuw and Driessen, 1999](#); [Hardin and Rocke, 2005](#); [Cerioli, 2010](#); [Ro et al., 2015](#); [Li et al., 2024](#)) can be applied to rescue additional observations as inliers ([Rousseeuw and Driessen, 1999](#)), such reweighting procedures requires the specification of a significance level that balances type-I error and power. Selecting the appropriate significance level or cut-off threshold complicates model selection. Another popular method for estimating the number of outliers is forward search ([Riani et al., 2009](#); [Atkinson et al., 2010](#)). Here new observations are gradually added to the selected subset. Unfortunately, forward search is designed for low-dimensional data and does not address the model selection in high-dimensional settings.

In a manner akin to *clustering instability* ([Wang, 2010](#); [Fang and Wang, 2012](#)), our bootstrap procedure estimates the instability of our  $h$ -subset selection algorithm. Stability is a prominent concept in statistics, proving effective in selecting regularization parameters ([Sun et al., 2013](#); [Wen et al., 2023](#)) and controlling false discoveries ([Meinshausen and Bühlmann, 2010](#); [Wang et al., 2011](#)). To our knowledge, this is the first application of stability in the context of high-dimensional outlier detection. We find that the subset size exhibiting minimal instability almost always corresponds to the true number of inliers. Consequently, the selected  $h$ -subset discriminates between outliers and inliers in a data-driven, nonparametric, and robust manner, eliminating the need for a predefined significance level. Moreover, the instability path provides insights into the distribution of outliers. For example, a redescending instability path suggests the presence

of an outlier masking effect, where extreme outliers overshadow the intermediate ones.

## 2 Background

Given a multivariate data matrix  $X \in \mathbb{R}^{n \times p}$ , assume that most of the observations are sampled from a unimodal distribution with mean  $\mu \in \mathbb{R}^p$  and covariance  $\Sigma \in \mathbb{R}^{p \times p}$ . Simultaneously suppose that there exists a subset of outliers markedly diverging from the primary mode. For the purpose of outlier detection and robust estimation, we are interested in finding a subset  $H \subset \{1, 2, \dots, n\}$  of size  $h$  that is outlier-free. The mean and covariance estimated from the subset are given by

$$\hat{\mu} = \frac{1}{h} \sum_{i \in H} x_i \quad \text{and} \quad \hat{\Sigma} = \frac{1}{h} \sum_{i \in H} (x_i - \hat{\mu})(x_i - \hat{\mu})^\top, \quad (1)$$

where the  $x_i \in \mathbb{R}^p$  are the rows of  $X$  indexed by the integer subset  $H$ .

**Definition 2.1.** *The minimum covariance determinant problem seeks the  $h$  observations from  $x_1, x_2, \dots, x_n$  minimizing the determinant of  $\hat{\Sigma}$  defined in equation (1).*

Rousseeuw and Driessen (1999) proposed the first computationally efficient algorithm (FastMCD) to tackle the MCD problem. Starting from a random initial subset  $H$ , FastMCD first obtains an initial estimate of  $\mu$  and  $\Sigma$  via equation (1). Then, based on the Mahalanobis distances

$$d_i = \sqrt{(x_i - \hat{\mu})^\top \hat{\Sigma}^{-1} (x_i - \hat{\mu})}, \quad (2)$$

the observations  $x_i, i = 1, 2, \dots, n$  are ranked from closest to furthest. In the remaining part of the paper, we may also write  $\text{MD}(x_i; \hat{\mu}, \hat{\Sigma})$  to denote the Mahalanobis distance (2). Given the permutation  $\pi$  producing the ranking  $d_{\pi(1)} \leq d_{\pi(2)} \leq \dots \leq d_{\pi(n)}$ ,  $H$  is updated as

$$H = \{\pi(1), \pi(2), \dots, \pi(h)\}. \quad (3)$$

Rousseeuw and Driessen (1999) call the combination of procedures (1), (2), and (3) a concentration step (C-step). Invoking a uniqueness property (Grübel, 1988), Rousseeuw and Driessen (1999) show that each concentration step monotonically decreases  $\det(\hat{\Sigma})$ .

## 2.1 Statistical Depth

Statistical depth is a nonparametric notion commonly used to rank multivariate data from a center outward (Zuo and Serfling, 2000a; Zhang et al., 2023). A statistical depth function increases with the centrality of the observation, with values ranging between 0 and 1. After computing the statistical depth of all observations within a data set, it is natural in estimating means and covariances to retain the  $h$  observations with the greatest depths. Zhang et al. (2023) investigated the application of two representative depth notions, projection depth and  $L_2$  depth (Zuo and Serfling, 2000a). Their experiments demonstrate that projection depth is more robust across different simulation settings. Projection depth has the added benefit of being affine invariant (Zuo and Serfling, 2000a; Zuo, 2006). Therefore, we focus on projection depth as our primary depth notion.

**Definition 2.2.** *The projection depth of a vector  $x \in \mathbb{R}^p$  with respect to a distribution  $F$  is defined as*

$$D(x; F) = \left[ 1 + \sup_{\|u\|=1} \frac{|u^\top x - \text{med}(u^\top y)|}{\text{MAD}(u^\top y)} \right]^{-1}, \quad (4)$$

where  $y$  is a multivariate random variable that follows the distribution  $F$ ,  $\text{med}(V)$  is the median of a univariate random variable  $V$ , and  $\text{MAD}(V) = \text{med}(|V - \text{med}(V)|)$  is the median absolute deviation from the median.

Since there exists no closed-form expression for the quantity (4), in practice projection depth is approximated by generating  $k$  random directions  $u$ . For the purpose of ranking the observations from a center outward, one can compute  $D(x_i; \hat{F}_n)$  for  $i$  between 1 and  $n$ , where  $\hat{F}_n$  is the empirical distribution of  $X \in \mathbb{R}^{n \times p}$ . In this case projection depth is also referred to as sample projection depth. We write  $D(x_i; \hat{F}_n)$  as  $D(x_i; X)$  to highlight its dependence on the observed data matrix  $X$ . Sample projection depths are generally efficient to compute with a time complexity of  $O(nkp)$ . In the R computing environment, the package `dda1pha` (Lange et al., 2014; Pokotylo et al., 2016) efficiently delivers sample projection depths.

## 2.2 Reweighted Estimators

Many MCD algorithms employ reweighting to avoid excluding too many observations. For example, the fast depth-based (FDB) algorithm of Zhang et al. (2023) operates by: (a) computing statistical depths and defining the initial  $h$ -subset to be the  $h$  observations

with the largest depths (b) computing  $\hat{\mu}$  and  $\hat{\Sigma}$  by equation (1), and (c) re-estimating  $\hat{\mu}$  and  $\hat{\Sigma}$  via the reweighting scheme (5) of Rousseeuw and Driessen (1999). In summary,

$$c = \operatorname{med}_i \frac{\mathcal{D}^2(x_i; \hat{\mu}, \hat{\Sigma})}{\chi_{p,0.5}^2}, \quad w_i = \begin{cases} 1 & \mathcal{D}^2(x_i; \hat{\mu}, c\hat{\Sigma}) \leq \chi_{p,0.975}^2 \\ 0 & \mathcal{D}^2(x_i; \hat{\mu}, c\hat{\Sigma}) > \chi_{p,0.975}^2, \end{cases} \quad (5)$$

$$\hat{\mu}_{\text{re}} = \frac{\sum_{i=1}^n w_i x_i}{\sum_{i=1}^n w_i}, \quad \hat{\Sigma}_{\text{re}} = \frac{\sum_{i=1}^n w_i (x_i - \hat{\mu}_{\text{re}})(x_i - \hat{\mu}_{\text{re}})^\top}{\sum_{i=1}^n w_i - 1}.$$

Here  $\mathcal{D}(x_i; \hat{\mu}, \hat{\Sigma})$  is the Mahalanobis distance of  $x_i$  from the center  $\hat{\mu}$ . FDB amends the depth-induced  $h$ -subset to include observations with weight 1 and skips concentration steps altogether. In practice, a reweighting procedure like (5) with a subjectively chosen cut-off value may underestimate or overestimate the number of outliers.

## 3 Methods

### 3.1 Spectral Embedding

A key ingredient of our attack on MCD is to transform the data to principal component scores before best subset selection. We first center the data matrix  $X \in \mathbb{R}^{n \times p}$  and then compute the singular value decomposition  $\tilde{X} = USV^T$  of the centered data  $\tilde{X}$ , where  $V \in \mathbb{R}^{p \times \min\{n,p\}}$ , and  $S$  has diagonal entries in decreasing order. Finally we select the first  $q$  principal components  $Z = \tilde{X}V[:, 1 : q]$ . The matrix  $Z$  is the substrate from which we identify the best  $h$ -subset. It is also common practice to normalize the variables of the data matrix to have unit variance before performing principal component analysis. This action also makes our algorithm scale invariant. However, we find empirically that rescaling is unnecessary in outlier detection. Therefore for the sake of simplicity we choose to omit normalization.

We call the general theme of performing MCD after spectral embedding a spectral minimum covariance determinant problem (SpectralMCD). An important observation is that when  $q = p$ , the principal component matrix is invertible, and since the MCD problem is affine invariant (Rousseeuw and Driessen, 1999), SpectralMCD in that case will be equivalent to the regular MCD. This implies that the spectral minimum covariance determinant problem includes the MCD problem as a special case. If we properly choose the number of principal components, then SpectralMCD should be at least as powerful as

MCD in outlier detection if  $p < n$ , albeit at the cost of more computation. Fortunately, we demonstrate that a good choice can be achieved via algorithm instability as introduced in [Section 3.3](#). As noted in [Section 2.1](#), the time complexity for computing sample projection depths for a data set of size  $n \times p$  is  $O(nkp)$ . Spectral embedding automatically alleviates the computational burden in estimating projection depth by reducing  $p$  to  $q$ .

## 3.2 Concentration Steps

When the specified subset size  $h$  is close to the true number of inliers and projection depth is difficult to approximate, depth-induced  $h$ -subsets may still contain several outliers. The FDB algorithm of [Zhang et al. \(2023\)](#), which skips concentration steps, is able to work well despite possible outliers in the initial  $h$ -subset because the reweighting step (5) adds an additional layer of projection. Unfortunately, the reweighting step (5) itself may be detrimental to outlier detection if the cut-off value is not properly chosen. Moreover, when  $p > n$ , the reweighting step is stymied by the singularity of the matrix  $\hat{\Sigma}$ . To ensure that the identified  $h$ -subset contains as few outliers as possible, we employ concentration steps as described in [Section 2](#) to further refine the  $h$ -subset.

## 3.3 Model Selection via Stability

In the MCD literature, selecting the right subset size  $h$  poses a consistent challenge. Although spectral embedding brings numerous advantages, determining the optimal number of principal components for outlier detection remains a hurdle. [Berenguer-Rico et al. \(2023\)](#) propose a normality based test statistic to determine the subset size in the related but different problem of least trimmed squares. However, to our knowledge, there are

---

### Algorithm 1 Spectral Minimum Covariance Determinant (SpectralMCD)

---

**Input:** Data matrix  $X \in \mathbb{R}^{n \times p}$ , subset size  $h < n$ , number of principal components  $q \leq \min\{n, p\}$ , number of random directions  $k$ .

- 1: Center  $X$  to obtain  $\tilde{X}$  and compute the singular value decomposition  $\tilde{X} = USV^T$ .
- 2: Compute the principal components matrix  $Z = \tilde{X}V[:, 1 : q]$  and the projection depths  $d_i = D(z_i; Z)$ ,  $i = 1, 2, \dots, n$ , using  $k$  random directions.
- 3: Sort  $d_i$  in decreasing order, yielding permutation  $\pi$  with  $d_{\pi(1)} \geq d_{\pi(2)} \geq \dots \geq d_{\pi(n)}$ . Set  $H = \{\pi(1), \pi(2), \dots, \pi(h)\}$ .
- 4: Update  $H$  using regular concentration steps (1), (2), and (3) on the principal component matrix  $Z$  until  $H$  stabilizes.

**Output:** The best  $h$ -subset  $H$

---

no options for determining the appropriate subset size in the MCD problem other than reweighting (Rousseeuw and Driessen, 1999) and forward search (Riani et al., 2009). Drawing inspiration from the notion of *clustering instability* (Wang, 2010; Fang and Wang, 2012), we now describe a bootstrap procedure for estimating both the number of inliers  $h$  (equivalently the number of outliers  $n - h$ ) and the appropriate number of principal components  $q$ . The task of robust location/scatter estimation can be viewed as a special case of clustering with two clusters, with one cluster consisting of inliers, and the other cluster consisting of outliers. Unlike traditional clustering, the outlier cluster does not necessarily exhibit spatial structure. This spatial ambiguity causes classic strategies in clustering, such as the gap statistic (Tibshirani et al., 2001), to fail. If the number of inliers  $h$  is suitably chosen, then different bootstrapped samples should yield similar conclusions about which cases are outliers in the data matrix  $X$ . Suppose the bootstrapped samples  $\dot{X}$  and  $\ddot{X}$  deliver indicator functions (binary maps)  $\psi_1$  and  $\psi_2$  distinguishing outliers from inliers, with a value of 1 denoting an outlier and a value of 0 denoting an inlier. To measure the distance between  $\psi_1$  and  $\psi_2$ , we resort to the probability that  $\psi_1$  and  $\psi_2$  do not agree on observations randomly selected from  $X$ .

**Definition 3.1.** *The probability distance between two binary maps  $\psi_1$  and  $\psi_2$  on a data matrix  $X$  is*

$$p_X(\psi_1, \psi_2) = \frac{1}{n} \sum_{i=1}^n |\psi_1(x_i) - \psi_2(x_i)|. \quad (6)$$

The distance  $p_X(\psi_1, \psi_2)$  can be interpreted as the probability of the symmetric difference of the two outlier sets encoded by the binary maps. The following standard definition of clustering instability (Wang, 2010) allows for  $K > 2$  clusters.

**Definition 3.2.** *The clustering distance between two clusterings  $\psi_1$  and  $\psi_2$  on the data matrix  $X$  is*

$$d_X(\psi_1, \psi_2) = \frac{1}{n^2} \sum_{i=1}^n \sum_{j=1}^n |I_{\psi_1(x_i)=\psi_1(x_j)} - I_{\psi_2(x_i)=\psi_2(x_j)}|, \quad (7)$$

where  $\psi_1$  and  $\psi_2$  map an arbitrary vector  $x \in \mathbb{R}^p$  to a cluster label  $k \in \{0, 1, \dots, K - 1\}$ .

The next proposition elucidates the connection between probability distance and clustering distance given just two clusters.

**Theorem 3.1.** *When there is only two clusters ( $K = 2$ ), the two distances covered by Definition 3.1 and Definition 3.2 satisfy*

$$d_X(\psi_1, \psi_2) = 2p_X(\psi_1, \psi_2)[1 - p_X(\psi_1, \psi_2)].$$



[Theorem 3.1](#) reduces the computational complexity of computing  $d_X(\psi_1, \psi_2)$  from  $O(n^2)$  to  $O(n)$ . This saves computation time when  $n$  is large. Proof of [Theorem 3.1](#) is available in the supplement.

[Haslbeck and Wulff \(2020\)](#) observe that clustering distance can be adversely affected by differences in cluster sizes. In our context, both  $p_X(\psi_1, \psi_2)$  and  $d_X(\psi_1, \psi_2)$  becomes problematic when  $h$  approaches  $n$  because there is then little room for the binary mappings  $\psi_1$  and  $\psi_2$  to disagree. For example, in the extreme situation  $h = n$ , both measures will be 0. To adjust for the effect of cluster sizes in  $p_X(\psi_1, \psi_2)$ , we employ the scaled metric

$$p_X^c(\psi_1, \psi_2) = \frac{1}{c} p_X(\psi_1, \psi_2) \quad (8)$$

where  $c = 2 \frac{h}{n} \frac{(n-h)}{n}$  is the expectation of  $|\psi_1(x_i) - \psi_2(x_i)|$  when  $\psi_1$  and  $\psi_2$  represent two randomly chosen inlier sets of size  $h$  from the rows of  $X$ . [Sun et al. \(2013\)](#) adopt a similar scaling technique for tuning parameter selection in penalized regression. For a measure of instability based on clustering distance, we follow [Haslbeck and Wulff \(2020\)](#) and employ the metric

$$d_X^c(\psi_1, \psi_2) = \frac{d_X(\psi_1, \psi_2)}{2c'(1-c')} - 1, \quad (9)$$

where  $c' = [ \binom{h}{2} + \binom{n-h}{2} ] / \binom{n}{2}$ . The supplement gives the derivation of (9) and demonstrates that  $c = 2 \frac{h}{n} \frac{(n-h)}{n}$  is asymptotically equal to  $1 - c'$  as  $n$  and  $h$  tend to infinity. Therefore, the two scaled distances are roughly comparable.

The average

$$\hat{s}(h, q) = \frac{1}{B} \sum_{i=1}^B d_X^c(\psi_{1,b}, \psi_{2,b}) \quad (10)$$

across  $B$  independent bootstrap pairs is our final measure of algorithmic instability. Here the binary maps  $\psi_{1,b}$  and  $\psi_{2,b}$  are subscripted by the bootstrap pair index  $b$ . [Algorithm 2](#) illustrates the workflow of our instability estimation algorithm using (9) as the dissimilarity measure and (10) as the instability measure. The general idea is to search over a pre-set collection of pairs  $(h, q)$  to identify a parameter combination with minimal instability. We choose projection depth over Mahalanobis distance to distinguish inliers from outliers since it's decision boundary is not strictly elliptical which allows for more flexibility. Additionally, we empirically found that projection depth is less affected by extreme outliers compared with Mahalanobis distance. Although [Algorithm 2](#) appears computationally intensive at first glance, many computational results can be recycled

during a grid search. Specifically, we only need to compute the singular value decomposition and principal component projection once per bootstrap sample. For  $q$  fixed, the computed projection depths can be used for all values of  $h$ . Further optimization for computing projection depths is possible.

---

**Algorithm 2** Instability Estimation

---

**Input:** Data matrix  $X \in \mathbb{R}^{n \times p}$ , subset size  $h < n$ , number of principal components  $q \leq \min\{n, p\}$ , number of random directions  $k$ , number of bootstrap pairs  $B$ .

- 1: **for**  $b = 1 : B$  **do**
- 2:   Construct a pair of bootstrapped samples  $\dot{X}_b$  and  $\ddot{X}_b$ .
- 3:   Apply [Algorithm 1](#) to  $\dot{X}_b$  and  $\ddot{X}_b$  to obtain best  $h$ -subsets  $\dot{H}_b$  and  $\ddot{H}_b$ . As by-products, store the column means  $\dot{\mu}_b$  and  $\ddot{\mu}_b$  of  $\dot{X}_b$  and  $\ddot{X}_b$ , the right singular matrices  $\dot{V}_b$  and  $\ddot{V}_b$ , and the principal components  $\dot{Z}_b$  and  $\ddot{Z}_b$ .
- 4:   Center and right multiply  $X$  by  $(\dot{\mu}_b, \dot{V}_b[:, 1 : q])$  and  $(\ddot{\mu}_b, \ddot{V}_b[:, 1 : q])$  respectively to obtain  $\dot{Z}$  and  $\ddot{Z}$ .
- 5:   Compute projection depths  $\dot{d}_i = D(\dot{z}_i; \dot{Z}_b[\dot{H}_b, ])$ ,  $\ddot{d}_i = D(\ddot{z}_i; \ddot{Z}_b[\ddot{H}_b, ])$ ,  $i = 1, 2, \dots, n$  with  $k$  random directions.
- 6:   Set  $\psi_{1,b}(x_i) = 0$  if  $\dot{d}_i$  is within the  $h$ -largest and  $\psi_{1,b}(x_i) = 1$  otherwise.  $\psi_{2,b}(x_i)$  is defined similarly.
- 7:   Compute  $d_X^c(\psi_{1,b}, \psi_{2,b})$  by equation (9).
- 8: **end for**

**Output:**  $\hat{s}(h, q)$  in (10).

---

## 4 Simulation Studies

In this section, we compare our method (SpectralMCD) to minimum regularized covariance determinant (MRCD) ([Boudt et al., 2020](#)) and FDB ([Zhang et al., 2023](#)) for the under-determined case ( $p > n$ ). Code for our method and experiments is available at <https://github.com/qhengncsu/StableMCD>. We note that our framework also works well for the over-determined case ( $p < n$ ), but due to the limitation of space, we focus on the high-dimensional case and defer experiments where  $p < n$  to the supplement. Since the sample covariance matrix is singular when  $p > n$ , and FDB’s reweighting step must be skipped. In other words, FDB reduces to finding the  $h$  observations with greatest projection depths. We adopt the simulation protocol of [Boudt et al. \(2020\)](#), but extend  $p$  beyond the range previously considered. Without loss of generality, we set the mean vector  $\mu \in \mathbb{R}^p$  to 0. The covariance matrix  $\Sigma$  is constructed iteratively to ensure that its condition number (CN) closely approximates 50. Section 4 of ([Agostinelli et al., 2015](#)) explains in detail this covariance matrix generation protocol. Our simulated outliers are

Table 1: Simulation results when  $p = 500$ , all metrics are averaged over 50 replicates.

		10%			25%			40%		
		FN	F1	time	FN	F1	time	FN	F1	time
$l = 1$	MRCD	0	0.33	117	0	0.67	128	0	0.53	140
	FDB	0	0.33	2	0	0.67	2	48	0.89	2
	SpectralMCD	0	1	63	0	1	67	0	1	73
$l = 5$	MRCD	0	0.33	137	0	0.67	135	0	0.89	125
	FDB	0	0.33	2	0	0.67	2	0	0.89	2
	SpectralMCD	0	1	70	0	1	71	0	1	64
$l = 20$	MRCD	0	0.33	134	0	0.67	172	0	0.89	136
	FDB	0	0.33	2	0	0.67	2	0	0.89	2
	SpectralMCD	0	1	71	0	1	89	0	1	70

generated from the distribution  $\mathcal{N}(50a, \Sigma)$ , where  $a$  is an eigenvector of  $\Sigma$ . We randomly sample  $a$  from the  $l$  eigenvectors that corresponds to the  $l$  smallest eigenvalues of  $\Sigma$ . This setup is intentionally crafted so that the direction  $a$  poses the greatest difficulty in outlier detection. We note that (Boudt et al., 2020) considers only the case where  $l = 1$ . We find that a PCA with just 2 principal components already handles this set-up very well. Here we also consider the more challenging case where  $l = 5$  and  $l = 20$ , such that more than 2 principal components are needed to identify the outliers. Empirically, a general rule-of-thumb appears to be we need one principal component for each outlier direction.

We put  $h = \lfloor 0.5n \rfloor$  for the two baseline methods since they lack a mechanism for calibrating the subset size  $h$  in the high-dimensional case when  $p > n$ . For our workflow, we first apply Algorithm 2 to search over the grid  $h = \lfloor 0.5n \rfloor, \lfloor 0.55n \rfloor, \dots, \lfloor 0.95n \rfloor$  and  $q = 2, 10, 50$ . We note that the grid for  $q$  does not match the number of possible outlier directions. This is to demonstrate that Spectral MCD can still work well even if the number of principal components are moderately over-specified. We use FN (number of false negatives in outlier detection), and the F1 score to measure of accuracy of outlier detection. We use computation time (in seconds) to measure the efficiency. We note that the computation time for SpectralMCD includes the time used in the bootstrap procedure to identify the optimal parameter combination. For MRCD and FDB, we label observations that are not included in the  $h$ -subset as outliers. We set  $n = 300$  and consider both  $p = 500$  and  $p = 1000$ . The outlier ratios are set at 10%, 25%, and 40%. Table 1 and Table 2 presents the simulation results when  $p = 500$  and  $p = 1000$ , respectively. illustrates the instability paths using  $p = 500$ ,  $l = 20$ , and in the presence of 25% of outliers. Our work flow appears to be able to correctly identify the proportion

Table 2: Simulation results when  $p = 1000$ , all metrics are averaged over 50 replicates.

		10%			25%			40%		
		FN	F1	time	FN	F1	time	FN	F1	time
$l = 1$	MRCD	0	0.33	153	0	0.67	217	0	0.51	365
	FDB	0	0.33	8	0.2	0.67	9	51	0.89	14
	SpectralMCD	0	1	269	1	1	299	0	1	554
$l = 5$	MRCD	0	0.33	216	0	0.67	198	0	0.89	248
	FDB	0	0.33	9	0	0.67	9	0	0.89	11
	SpectralMCD	0	1	294	0	1	289	0	1	434
$l = 20$	MRCD	0	0.33	355	0	0.67	377	0	0.89	330
	FDB	0	0.33	10	0	0.67	10	0	0.89	10
	SpectralMCD	0	1	366	0	1	364	0	1	340

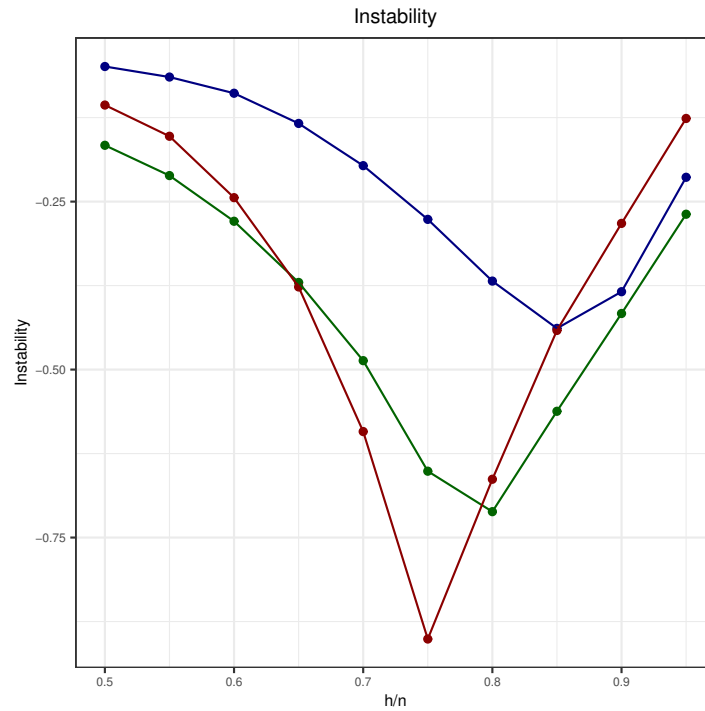


Figure 1: Instability path visualization for simulated data when  $p = 500$ ,  $l = 20$ , and there are 25% of outliers. The blue, green, red lines are instability paths at  $q = 2$ ,  $q = 10$ ,  $q = 50$ .

of inliers for every single scenario and replicate, and maintains a perfect F1 score. As commented earlier, both MRCD and FDB lack a mechanism for calibrating  $h$  when  $p > n$ , so that with  $h$  chosen conservatively at  $\lfloor 0.5n \rfloor$ , they produce a surplus of false positives in outlier detection. In general, FDB is lightning quick compared to the other two methods. However, when the outlier proportion reaches 40% at  $l = 1$ , it unfortunately breaks down and yields large estimation errors. Although our workflow is also based on projection depth, it remains robust in this particular setting through using the principal component transform to reveal the hidden low-dimensional structure of the data. The computation time of MRCD scales cubically with  $p$ . As a result, when  $p$  grows sufficiently large, our workflow becomes more efficient than MRCD, even though we invoke a costly bootstrap procedure to search for the best parameter combination.

## 5 Real Data Examples

### 5.1 Fruit Spectral Data

Our first real data example, referred to as the fruit data, comprises spectra from three distinct cantaloupe cultivars, labeled D, M, and HA with sample sizes of 490, 106, and 500, respectively. Originally introduced by [Hubert and Van Driessen \(2004\)](#) and later examined by [Hubert et al. \(2012\)](#), these data encompass 1096 total observations recorded across 256 wavelengths. [Hubert and Van Driessen \(2004\)](#) note that the cultivar HA encompasses three distinct groups derived from various illumination systems. Unfortunately, the assignment of individual observations to specific subgroups and the potential impact of the subgroups on spectra is unavailable.

Our purpose is to estimate the number of outliers and decide which observations qualify as outliers. FDB with  $h = \lfloor 0.5n \rfloor$  is our the baseline method. As in [Section 3.3](#), an observation  $x_i$  is flagged by FDB as an outlier when  $w_i$  in the reweighting step [\(5\)](#) equals 0. For our method, we applied [Algorithm 2](#) over the grid  $h = \lfloor 0.5n \rfloor, \lfloor 0.55n \rfloor, \dots, \lfloor 0.95n \rfloor$  with  $q = 2$  principal components. The grid search over 50 bootstrap pairs took 24 seconds to complete. We then applied [Algorithm 1](#) to identify the inliers and outliers using the optimal parameter combination. The choice of  $q = 2$  is motivated by a scree plot demonstrating that nearly all variance can be explained using just two principal components ([Hubert et al., 2012](#)).

[Figure 2](#) depicts the experimental outcomes. The left panel of [Figure 2](#) shows the first

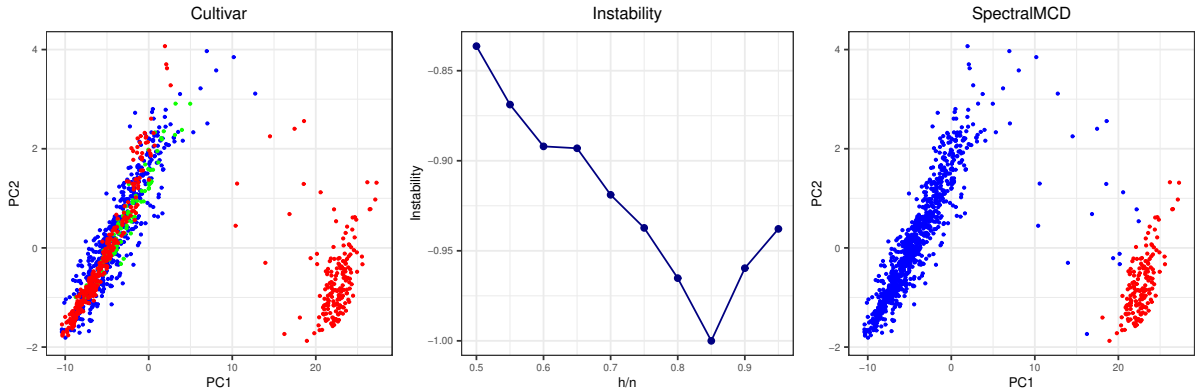


Figure 2: Experimental results for the fruit data set. In the left panel, cultivar D points are colored blue, cultivar M points are colored green, and cultivar HA points are colored red. In the right panel, blue points are inliers while red points are outliers.

two principal components of the data set, with each point colored by the corresponding cultivar. Evidently, observations significantly diverging from the primary mode almost exclusively belong to the HA cultivar. The middle panel displays the instability path computed by [Algorithm 2](#), which is minimized at  $h = \lfloor 0.85n \rfloor$ . The right panels illustrate the assignment of inliers and outliers identified by SpectralMCD based on the parameter combination  $(h = \lfloor 0.85n \rfloor, q = 2)$ . SpectralMCD appears quite effective in segregating the two modes, although there are a few points far away from the primary mode that are not assigned as outliers. This might be due to the fact that our search grid is not fine grained enough. FDB in this example categorizes 497 points as outliers using a cut-off of 0.975, which is hard to interpret given the principal component visualization. We suspect that the reweighting procedure [\(5\)](#) might have failed due to the ill conditioning of the estimated covariance matrix. [Algorithm 2](#) estimates approximately  $1096 \times 0.15 \approx 164$  outliers, roughly a third of the 500 observations. We conjecture that the outliers in the HA cultivar correspond to a subgroup with a distinctive illumination pattern.

## 5.2 Glass Spectral Data

Our second real data example consists of EPXMA spectra over  $p = 750$  wavelengths collected on 180 different glass samples ([Lemberge et al., 2000](#)). These data were analyzed via robust principal component analysis in [Hubert et al. \(2005\)](#). In [\(Hubert et al., 2005\)](#), 3 principal components were chosen using the rationale that it explains 99% of the variance (or 96% of the robust variance). However, as we demonstrate in the next subsection, using the proportion of variance explained to select the appropriate number of principal

components is not always reliable. More specifically, in [Section 5.3](#), the first 2 principal components only explains around 40% of the variance, but using 2 principal components turns out to be the most effective in outlier detection. Here we search over the 2D parameter grid  $h = \lfloor 0.5n \rfloor, \lfloor 0.525n \rfloor, \dots, \lfloor 0.975n \rfloor$  and  $q = 2, 3, 10$ . The grid search took 86 seconds to complete. We see from [Figure 3](#) that at  $q = 2$ , instability is minimized at  $h = \lfloor 0.775n \rfloor$ . However, at  $q = 3$  and  $q = 10$ , instability is minimized at  $\lfloor 0.625n \rfloor$  and  $\lfloor 0.6n \rfloor$ , respectively. Out of all three instability paths, the minimum is attained at  $(q = 3, h = \lfloor 0.625n \rfloor)$ , but the instability at  $(q = 10, h = \lfloor 0.6n \rfloor)$  is nearly identical. We observed that incorporating additional principal components exposed more outliers that were not identified when using only two principal components, as shown in the middle and right panels of [Figure 3](#). We note that [Hubert et al. \(2005\)](#) used  $h = \lfloor 0.7n \rfloor$  and identified around 28% of observations as outliers. Here our instability framework also favors the choice of 3 principal components, but our instability framework suggests there are more outliers than concluded by [Hubert et al. \(2005\)](#). We also see that at  $q = 3$ , the instability path exhibits a dip at  $h = \lfloor 0.925n \rfloor$ . This hints at the existence of a few extreme outliers that overshadows the intermediate ones so that the algorithm will relatively stably select those outliers at  $h = \lfloor 0.925n \rfloor$ .

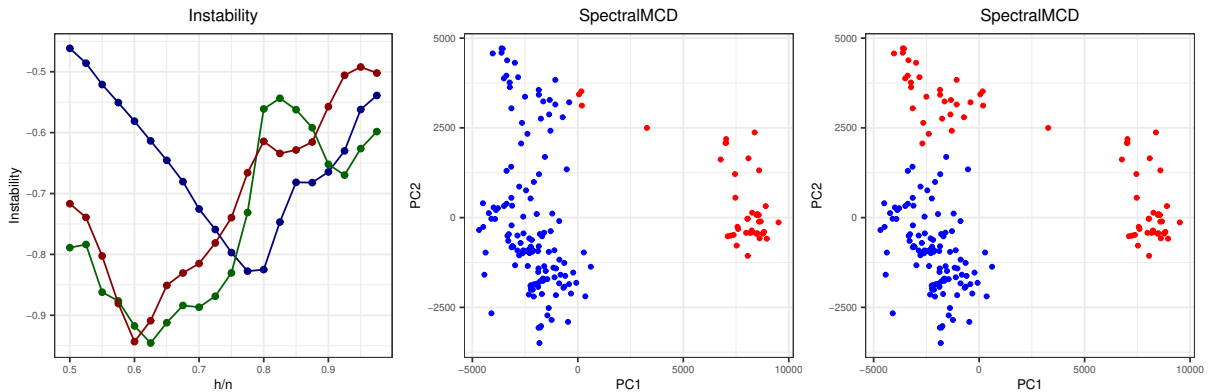


Figure 3: Experimental results for the glass spectra data set. In the left panel, blue, green, red lines are instability paths at  $q = 2$ ,  $q = 3$ ,  $q = 10$ , respectively. Middle panel shows inlier/outlier classification using  $(q = 2, h = \lfloor 0.775n \rfloor)$ . Right panel shows inlier/outlier classification using  $(q = 3, h = \lfloor 0.625n \rfloor)$ .

### 5.3 Breast Cancer Data

Our third real data example comes from the The Cancer Genome Atlas (TCGA) project ([Network, 2012](#)). The breast cancer project (TCGA-BRCA) encompasses approximately

1100 patients with invasive carcinoma of the breast. Our data is sourced from cBioPortal at <https://www.cbioportal.org/> (Cerami et al., 2012). We focus on the mRNA expression profiles of the patients. These profiles represent expression levels for 20531 genes on the 1100 samples. After performing a  $\log_2(x + 1)$  transform on the expression levels, we retained the top 2000 most variable genes. Apart from expression profiles, the data also record the estrogen receptor (ER) status of each sample. Women with estrogen receptor negative status (ER-) are typically diagnosed at a younger age and have a higher mortality rate (Bauer et al., 2007). Out of 1100 samples, 812 are estrogen receptor positive, 238 are negative, 48 are indeterminate, and 2 are missing. We retain the 1050 samples for which the estrogen receptor status is either positive or negative. Thus, our preprocessed data matrix has dimension  $1050 \times 2000$ .

As in Section 5.1, we first applied Algorithm 2 to estimate the proportion of outliers in the data set. We searched via Algorithm 2 over a two-dimensional parameter grid  $q = 2, 10, 100$  and  $h = \lfloor 0.5n \rfloor, \lfloor 0.55n \rfloor, \dots, \lfloor 0.95n \rfloor$ . The grid search takes 968 seconds to complete. We then applied Algorithm 1 to identify the outliers under the optimal parameter combination. Figure 4 depicts the experimental results. At  $q = 2$  and 10,

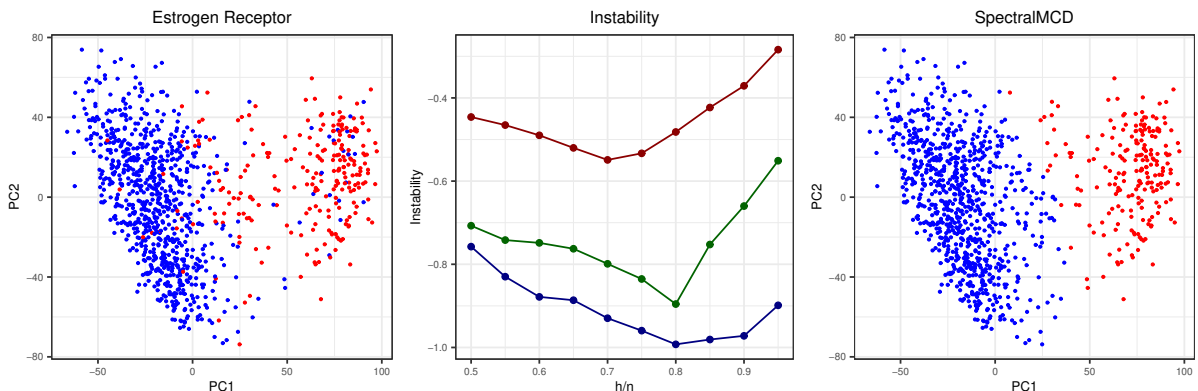


Figure 4: Experimental results for the breast cancer data set. In the left panel, blue points are estrogen receptor positive, red points are negative. In the middle panel, the blue, green, red lines are instability paths at  $q = 2$ ,  $q = 10$ ,  $q = 100$ . In the right panel, the blue points are inliers while red points are outliers.

the instability is minimized at  $h = \lfloor 0.8n \rfloor$ . However, at  $q = 100$ , the instability is minimized at  $h = \lfloor 0.7n \rfloor$ . Possibly the redundant principal components obscure the inlier/outlier structure. The optimal parameter combination is  $(h, q) = (\lfloor 0.8n \rfloor, 2)$ . In the general population, about 79-84% of breast cancer cases will be estrogen receptor positive (Allison et al., 2020). Our algorithms are able to infer this medical fact purely from the gene expression profile without reference to recorded estrogen receptor status.



Moreover, if we consider this problem as a binary classification problem, [Algorithm 1](#) achieves an unsupervised classification accuracy of 92.4%.

## 6 Discussion

This paper introduces a new method for model selection and outlier detection in the framework of the minimum covariance determinant (MCD) problem. We advocate principal components and minimum bootstrap instability as devices for uncovering the hidden low-dimensional structure of the inlier/outlier distribution. Instability paths constructed by the bootstrap method shed considerable light on the appropriate subset size  $h$  and number of principal components  $q$ . Projection depths also emerge as effective initiators for the MCD search process.

Our workflow is rigorously evaluated against well-established variants of the MCD algorithm, namely the fast depth-based (FDB) algorithm and the minimum regularized covariance determinant (MRCD) algorithm. In direct comparison on simulated data, our instability framework excels in accurately estimating the number of outliers and, by leveraging a larger portion of observations, in estimating location and scatter parameters. Several real-data sets likewise demonstrate the utility of instability paths in outlier detection. Here the findings are both revealing and reasonable. Finally, in high-dimensional scenarios, spectral embedding circumvents the computational burden of matrix inversions and enables faster overall execution than regularized MCD.

While proving effective in most settings, our instability framework is not a panacea for determining  $h$  in the MCD problem. We apply the proposed bootstrap procedure to univariate data and in the presence of outlier masking effect in the supplement. It is observed that our bootstrap procedure may not work well on univariate data, since in this setting bootstrapping may not introduce sufficient perturbations. In the presence of masking outliers, our instability path often exhibits a redescending shape. In that case, it is probably prudent to select  $h$  at the first trough instead of at minimal instability. In practice, we recommend combining instability paths with existing tools such as reweighting and residual diagnostic plots. Together, these methods provide the best insights. Although more research is surely needed, in our view instability paths constitute a valuable addition to the existing toolbox for outlier detection.

## Acknowledgements

We thank Seyoon Ko and Do Hyun Kim for useful suggestions. This research was partially funded by USPHS grants GM53275 and HG006139.

# A Proofs and Derivations

## A.1 Proof of Proposition 3.1

*Proof.* Let  $A$  and  $B$  denote the  $h$ -subsets selected by  $\psi_1$  and  $\psi_2$  from  $\{x_1, x_2, \dots, x_n\}$ . Suppose  $A\Delta B$  denotes the symmetric difference of the sets  $A$  and  $B$ . The binary map distance can be expressed as an expectation involving two independent random variables  $X$  and  $Y$  uniformly distributed over the set  $\{1, 2, \dots, n\}$ . In this context the distance between  $A$  and  $B$  amounts to

$$\begin{aligned}
d_X(\psi_1, \psi_2) &= \mathbb{E} [|I_A(X)I_A(Y) + I_{A^c}(X)I_{A^c}(Y) - I_B(X)I_B(Y) - I_{B^c}(X)I_{B^c}(Y)|] \\
&= \mathbb{E} \{ [I_A(X)I_A(Y) + I_{A^c}(X)I_{A^c}(Y) - I_B(X)I_B(Y) - I_{B^c}(X)I_{B^c}(Y)]^2 \} \\
&= \Pr(A)^2 + \Pr(A^c)^2 + \Pr(B)^2 + \Pr(B^c)^2 - 2\Pr(A \cap B)^2 \\
&\quad - 2\Pr(A \cap B^c)^2 - 2\Pr(A^c \cap B)^2 - 2\Pr(A^c \cap B^c)^2 \\
&= [\Pr(A \cap B) + \Pr(A \cap B^c)]^2 + [\Pr(A^c \cap B) + \Pr(A^c \cap B^c)]^2 \\
&\quad + [\Pr(A \cap B) + \Pr(A^c \cap B)]^2 + [\Pr(A \cap B^c) + \Pr(A^c \cap B^c)]^2 \\
&\quad - 2\Pr(A \cap B)^2 - 2\Pr(A \cap B^c)^2 - 2\Pr(A^c \cap B)^2 - 2\Pr(A^c \cap B^c)^2 \\
&= 2\Pr(A \cap B)\Pr(A \cap B^c) + 2\Pr(A^c \cap B)\Pr(A^c \cap B^c) \\
&\quad + 2\Pr(A \cap B)\Pr(A^c \cap B) + 2\Pr(A \cap B^c)\Pr(A^c \cap B^c) \\
&= 2[\Pr(A \cap B) + \Pr(A^c \cap B^c)]\Pr(A\Delta B) \\
&= 2[1 - \Pr(A\Delta B)]\Pr(A\Delta B).
\end{aligned}$$

We also provide a direct algebraic proof. Indeed,

$$\begin{aligned}
p_X(\psi_1, \psi_2)[1 - p_X(\psi_1, \psi_2)] &= \frac{1}{n} \sum_{i=1}^n |\psi_1(x_i) - \psi_2(x_i)| \left[ 1 - \frac{1}{n} \sum_{i=1}^n |\psi_1(x_i) - \psi_2(x_i)| \right] \\
&= \frac{1}{n^2} \sum_{i=1}^n |\psi_1(x_i) - \psi_2(x_i)| \sum_{i=1}^n [1 - |\psi_1(x_i) - \psi_2(x_i)|] \\
&= \frac{1}{n^2} \sum_{i=1}^n \sum_{j=1}^n |\psi_1(x_i) - \psi_2(x_i)| [1 - |\psi_1(x_j) - \psi_2(x_j)|]
\end{aligned}$$

Because

$$|\psi_1(x_i) - \psi_2(x_i)| = I_{\psi_1(x_i) \neq \psi_2(x_i)} \quad \text{and} \quad 1 - |\psi_1(x_j) - \psi_2(x_j)| = I_{\psi_1(x_j) = \psi_2(x_j)},$$

$$p_X(\psi_1, \psi_2)[1 - p_X(\psi_1, \psi_2)] = \frac{1}{n^2} \sum_{i=1}^n \sum_{j=1}^n I_{\psi_1(x_i) \neq \psi_2(x_i)} I_{\psi_1(x_j) = \psi_2(x_j)}.$$

By symmetry of  $(i, j)$ , we can also write

$$p_X(\psi_1, \psi_2)[1 - p_X(\psi_1, \psi_2)] = \frac{1}{n^2} \sum_{i=1}^n \sum_{j=1}^n I_{\psi_1(x_j) \neq \psi_2(x_j)} I_{\psi_1(x_i) = \psi_2(x_i)}.$$

Therefore

$$\begin{aligned} & 2p_X(\psi_1, \psi_2)[1 - p_X(\psi_1, \psi_2)] \\ = & \frac{1}{n^2} \sum_{i=1}^n \sum_{j=1}^n [I_{\psi_1(x_i) \neq \psi_2(x_i)} I_{\psi_1(x_j) = \psi_2(x_j)} + I_{\psi_1(x_j) \neq \psi_2(x_j)} I_{\psi_1(x_i) = \psi_2(x_i)}], \end{aligned}$$

and simple enumeration of all 16 possible choices of  $\psi_1(x_i)$ ,  $\psi_2(x_i)$ ,  $\psi_1(x_j)$ , and  $\psi_2(x_j)$  implies

$$I_{\psi_1(x_i) \neq \psi_2(x_i)} I_{\psi_1(x_j) = \psi_2(x_j)} + I_{\psi_1(x_j) \neq \psi_2(x_j)} I_{\psi_1(x_i) = \psi_2(x_i)} = |I_{\psi_1(x_i) = \psi_1(x_j)} - I_{\psi_2(x_i) = \psi_2(x_j)}|.$$

Thus, we have

$$d_X(\psi_1, \psi_2) = 2p_X(\psi_1, \psi_2)[1 - p_X(\psi_1, \psi_2)].$$

□

## A.2 Derivation of the Corrected Clustering Distance

We follow the arguments in [Haslbeck and Wulff \(2020\)](#). Under the simplifying assumption that  $\psi_1(x_i) = \psi_1(x_j)$  and  $\psi_2(x_i) = \psi_2(x_j)$  are equally likely for all pairs of  $(i, j)$ , symmetry entails

$$\begin{aligned} \mathbb{E}[d_X(\psi_1, \psi_2)] &= \mathbb{E}[|I_{\psi_1(x_i) = \psi_1(x_j)} - I_{\psi_2(x_i) = \psi_2(x_j)}|] \\ &= \mathbb{E}[I_{\psi_1(x_i) = \psi_1(x_j)} I_{\psi_2(x_i) \neq \psi_2(x_j)} + I_{\psi_1(x_i) \neq \psi_1(x_j)} I_{\psi_2(x_i) = \psi_2(x_j)}] \\ &= 2\mathbb{E}\{I_{\psi_1(x_i) = \psi_1(x_j)} [1 - I_{\psi_2(x_i) = \psi_2(x_j)}]\}, \end{aligned}$$

where the third equality is due to the symmetry of  $\psi_1$  and  $\psi_2$ . In view of the covariance identity  $E(XY) = E(X)E(Y) + \text{Cov}(X, Y)$ , we have

$$\begin{aligned} E\{\mathbf{I}_{\psi_1(x_i)=\psi_1(x_j)}[1 - \mathbf{I}_{\psi_2(x_i)=\psi_2(x_j)}]\} &= E[\mathbf{I}_{\psi_1(x_i)=\psi_1(x_j)}]E[1 - \mathbf{I}_{\psi_2(x_i)=\psi_2(x_j)}] \\ &+ \text{Corr}[\mathbf{I}_{\psi_1(x_i)=\psi_1(x_j)}, 1 - \mathbf{I}_{\psi_2(x_i)=\psi_2(x_j)}]\sqrt{\text{Var}[\mathbf{I}_{\psi_1(x_i)=\psi_1(x_j)}]}\sqrt{\text{Var}[1 - \mathbf{I}_{\psi_2(x_i)=\psi_2(x_j)}]}. \end{aligned}$$

Our Bernoulli event assumption implies that

$$\begin{aligned} E[\mathbf{I}_{\psi_1(x_i)=\psi_1(x_j)}] &= E[\mathbf{I}_{\psi_2(x_i)=\psi_2(x_j)}] = c' = \left[ \binom{h}{2} + \binom{n-h}{2} \right] / \binom{n}{2}, \\ \text{Var}[\mathbf{I}_{\psi_1(x_i)=\psi_1(x_j)}] &= \text{Var}[1 - \mathbf{I}_{\psi_2(x_i)=\psi_2(x_j)}] = c'(1 - c'). \end{aligned}$$

Thus, in estimating  $\text{Corr}[\mathbf{I}_{\psi_1(x_i)=\psi_1(x_j)}, 1 - \mathbf{I}_{\psi_2(x_i)=\psi_2(x_j)}]$ , it is reasonable to employ the metric

$$d_X^c(\psi_1, \psi_2) = \frac{d_X(\psi_1, \psi_2)}{2c'(1 - c')} - 1.$$

Observe that

$$1 - c' = 1 - \left[ \binom{h}{2} + \binom{n-h}{2} \right] / \binom{n}{2} = 1 - \frac{h(h-1) + (n-h)(n-h-1)}{n(n-1)},$$

and recall the definition of

$$c = \frac{2h(n-h)}{n^2} = 1 - \frac{h^2 + (n-h)^2}{n^2}$$

from equation (9) Since  $h^2 \asymp h(h-1)$ ,  $n^2 \asymp n(n-1)$ ,  $n^2 \asymp n(n-1)$ ,  $c$  and  $1 - c'$  are asymptotically equivalent and negligibly different when  $n$  and  $h$  are large.

## B Efficient Implementation of FastMCD

The main computational bottlenecks of the FastMCD algorithm are the concentration steps. These require repeated evaluation of the matrix inverse  $\Sigma^{-1}$  and determinant  $\det \Sigma$ . Here we describe a computational technique that limits these costly steps to the first iteration. In subsequent iterations,  $\Sigma^{-1}$  and  $\det \Sigma$  can be updated by the Sherman-Morrison formula and matrix determinant lemma.

Notice that in the multivariate setting, the Welford updates and downdates of the

sample mean  $\mu$  and the sample covariance matrix  $\Sigma$  become

$$\begin{aligned}\mu_{h+1} &= \frac{1}{h+1}(h\mu_h + y_{h+1}) \\ \mu_h &= \frac{1}{h}[(h+1)\mu_{h+1} - y_{h+1}] \\ \Sigma_{h+1} &= \frac{h}{h+1}\Sigma_h + \frac{1}{h}(y_{h+1} - \mu_{h+1})(y_{h+1} - \mu_{h+1})^\top \\ \Sigma_h &= \frac{h+1}{h}\Sigma_{h+1} - \frac{h+1}{h^2}(y_{h+1} - \mu_{h+1})(y_{h+1} - \mu_{h+1})^\top.\end{aligned}$$

Given that the update and downdate of  $\Sigma$  are rank-1 perturbations of  $\Sigma$ , we can invoke the Sherman-Morrison formula

$$(A + uv^\top)^{-1} = A^{-1} - \frac{A^{-1}uv^\top A^{-1}}{1 + v^\top A^{-1}u},$$

to update and downdate  $\Sigma^{-1}$ . We can also invoke the the matrix determinant lemma

$$\det(A + uv^\top) = \det(A(1 + v^\top A^{-1}u))$$

to update and downdate  $\det \Sigma$ .

More specifically, we update  $\Sigma_{h+1}^{-1}$  and  $\det \Sigma_{h+1}^{-1}$  via

$$\begin{aligned}\Sigma_{h+1}^{-1} &= \left(\frac{h+1}{h}\Sigma_h^{-1}\right) - \frac{(\frac{h+1}{h}\Sigma_h^{-1})(y_{h+1} - \mu_{h+1})(y_{h+1} - \mu_{h+1})^\top(\frac{h+1}{h}\Sigma_h^{-1})}{h + (y_{h+1} - \mu_{h+1})^\top(\frac{h+1}{h}\Sigma_h^{-1})(y_{h+1} - \mu_{h+1})} \\ \det \Sigma_{h+1} &= \frac{h}{h+1} \det \Sigma_h \left[1 + \frac{1}{h}(y_{h+1} - \mu_{h+1})^\top \left(\frac{h+1}{h}\Sigma_h^{-1}\right) (y_{h+1} - \mu_{h+1})\right].\end{aligned}$$

For the sake of brevity, we omit the similar downdates of  $\Sigma_h^{-1}$  and  $\det \Sigma_h^{-1}$ . At each concentration step, the new observations inserted into the  $h$ -subset are balanced by a like number of deletions of old observations.

## C Additional Experimental Results

### C.1 Univariate Data and Outlier Masking

In this section we investigate the performance of our bootstrap procedure on univariate data and address the ‘‘outlier masking’’ problem where some outliers are much more extreme than the intermediate outliers. This constitutes a classical challenge for outlier

detection methods. In the univariate case, we note that the MCD subset and the outlier mappings are computed differently. First, in the univariate case, we use the well-known exact computation algorithm (Rousseeuw and Leroy, 2005) for the MCD problem to find the best subset. Then an observation  $x_i$  is declared as an outlier if it not within the  $h$ -closest to the sample mean of the selected  $h$ -subset from the bootstrapped sample. We consider the following four settings:

- Setting 1:  $x_1, x_2, \dots, x_{800}$  are generated from  $\mathcal{N}(0, 1)$ ,  $x_{801}, x_{802}, \dots, x_{900}$  are generated from  $\mathcal{N}(-10, 1)$ , while  $x_{901}, x_{802}, \dots, x_{1000}$  are generated from  $\mathcal{N}(10, 1)$ .
- Setting 2:  $x_1, x_2, \dots, x_{800}$  are generated from  $\mathcal{N}(0, 1)$ ,  $x_{801}, x_{802}, \dots, x_{950}$  are generated from  $\mathcal{N}(5, 1)$ , while  $x_{951}, \dots, x_{1000}$  are generated from  $\mathcal{N}(1000, 1)$ .
- Setting 3: Same as setting 2, except that the observations are now two-dimensional.
- Setting 4: We adopt the simulation protocol of Section 4 in the paper using parameters  $n = 300, p = 500$  to generate the uncorrupted data. Then 15% of outliers are generated as  $\mathcal{N}(50a, \Sigma)$ , where  $a$  is the eigenvector that corresponds to the smallest eigenvalue of  $\Sigma$ . Additionally, 5% of outliers are generated as  $\mathcal{N}(5000b, \Sigma)$ , where  $b$  is the eigenvector corresponds to the second smallest eigenvalue of  $\Sigma$ .

Figure 5 visualizes the instability paths for all four settings. In particular, for setting 3 and 4, we use  $q = 2$  in Algorithm 2. For settings 1, our instability measure correctly identifies the true number of inliers/outliers ( $h = 800$ ) without ambiguity. For setting 2, unfortunately our bootstrap procedure fails to reveal the correct number of outliers with minimal instability, which is attained at  $h \in \{850, 900, 950\}$ . This anomaly likely arises because, in this setting, the outlier mapping process simplifies to sorting observations by their absolute deviation from the estimated mean. Therefore, as long as the estimated mean remains within a certain range, different bootstrapped samples will produce the same outlier mapping for the original data. In other words, bootstrapping does not introduce sufficient perturbation to alter the decision boundary. We believe that such degenerate data situations are rare in more than one dimensions. In general, our bootstrap procedure may have limited success with univariate data. In typical multivariate data, even when an outlier masking phenomenon occurs, the instability path will exhibit a double-descent shape. Both Setting 3 and Setting 4 in Figure 5 exemplify this assertion. Consequently, the instability path continues to provide valuable insights into

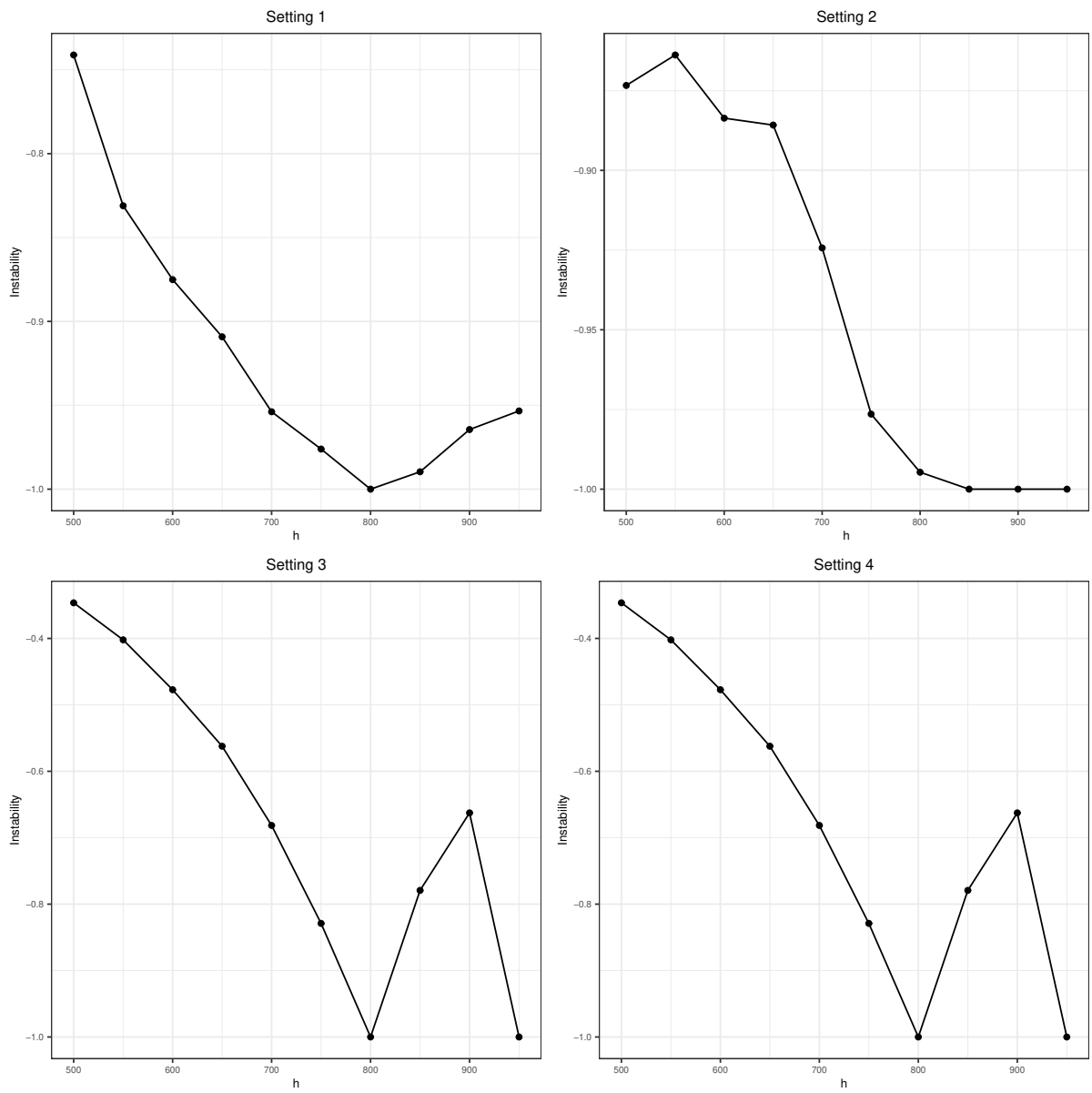


Figure 5: Instability paths for the settings 1, 2, 3, and 4, respectively. The sample points denote mean instability over 100 bootstrap pairs.



outlier detection. Should the instability path exhibits a prominent redescending shape, we recommend choosing  $h$  at the first trough instead of minimal instability.

## C.2 The Overdetermined Case $n < p$

In this section, we evaluate our workflow under the simulation protocol applied in the evaluation of both DetMCD (Hubert et al., 2012) and FDB (Zhang et al., 2023). The common protocol first generates inliers as  $x_i = Gy_i$ , where  $y_i$  is Gaussian  $\mathcal{N}(0, I_p)$ . The  $p \times p$  matrix  $G$  has diagonal elements equal to 1 and off-diagonal elements equal to 0.75. The protocol then generates potential outliers at contamination levels of 10%, 25%, and 40%. The outliers are categorized into four types depending on a scalar  $r$  that determines the separation between inlier and outlier clusters.

- Point outliers:  $y_i \sim \mathcal{N}(ra\sqrt{p}, 0.01^2I_p)$ , where  $\|a\| = 1$  and  $\sum_i a_i = 0$ .
- Cluster outliers:  $y_i \sim \mathcal{N}(rp^{-1/4}1, I_p)$ .
- Random outliers:  $y_i \sim \mathcal{N}(rp^{1/4}\nu_i/\|\nu_i\|, I_p)$ , where  $\nu_i \sim \mathcal{N}(0, I_p)$ .
- Radial outliers:  $y_i \sim \mathcal{N}(0, 5I_p)$ .

We set  $r = 5$  throughout this section. Point, Cluster, and Radial outliers were introduced by Hubert et al. (2012) and Random outliers by Zhang et al. (2023).

We omit comparison with DetMCD since the experiments of Zhang et al. (2023) demonstrate that FDB performs almost uniformly better than DetMCD. For FDB, we assume no prior knowledge of the number of outliers and conservatively equate  $h$  to  $\lfloor 0.5n \rfloor$ , the breakdown point for MCD estimators. For our method, we employ the following pipeline: (a) apply Algorithm 2 to search over the grid  $h = \lfloor 0.5n \rfloor, \lfloor 0.55n \rfloor, \dots, \lfloor 0.95n \rfloor$  and  $q \in \{2, p\}$  to pinpoint the parameter combination  $(\hat{h}, \hat{q})$  with the smallest average instability, (b) identify the optimal  $h$ -subset via Algorithm 1 based on  $(h, q) = (\hat{h}, \hat{q})$ , and (c) estimate  $\mu_X$  and  $\Sigma_X$  by the equation (1). We set the number of random directions to  $k = \max\{1000, 10q\}$ . The estimators for the data set  $Y$  are then obtained as  $\hat{\mu}_Y = G^{-1}\hat{\mu}_X$  and  $\hat{\Sigma}_Y = G^{-1}\hat{\Sigma}_X G^{-1}$ .

Our evaluation of the quality of these estimators relies on the following measures:

- $e_\mu = \|\hat{\mu}_Y - \mu_Y\|_2$ , where  $\mu_Y$  is the true mean vector of  $Y$ ; in this case  $\mu_Y = 0$ .
- $e_\Sigma = \log_{10}[\text{cond}(\hat{\Sigma}_Y \Sigma_Y^{-1})]$ , where  $\Sigma_Y$  is the true covariance matrix of  $Y$ , and the operator  $\text{cond}$  finds the condition number of a matrix. In this case  $\Sigma_Y = I_p$ .

- The Kullback–Leibler divergence

$$\text{KL}(\hat{\Sigma}_Y, \Sigma_Y) = \text{tr}(\hat{\Sigma}_Y \Sigma_Y^{-1}) - \log\{\det(\hat{\Sigma}_Y \Sigma_Y^{-1})\} - p.$$

We consider three combinations of  $n$  and  $p$ :  $(n, p) = (400, 40)$ ,  $(n, p) = (400, 80)$ , and  $(n, p) = (2000, 200)$ . [Table 3](#), [Table 4](#), [Table 5](#) show that our pipeline consistently offers more precise estimates than FDB, particularly in estimating  $\Sigma$ . Because SpectralMCD tries to incorporate as many observations as possible, its advantage becomes more pronounced as the proportion of outliers decreases. As  $p$  goes from 40 to 80, the performance of FDB deteriorates, and the comparative advantage of SpectralMCD becomes more evident. The deterioration of FDB might be due to the fact that the reweighting step (5) becomes less reliable as  $p$  grows. Additionally, it is evident that Algorithm 2 effectively selected the appropriate  $h$  across nearly all scenarios, except for the Point outliers scenario at a 40% outlier level. In this particular setting, both methods struggle to identify numerous outliers, and estimation is fraught with significant errors. We speculate that this specific setting is statistically impossible for MCD estimators. Finally, it is worth noting that while our pipeline yields more accurate estimates, it does so at the expense of a computationally intensive bootstrap procedure that takes considerably longer to run than the two baseline methods. Consult [Table 6](#) for specific timing comparisons.

## References

- Agostinelli, C., Leung, A., Yohai, V. J., and Zamar, R. H. (2015), “Robust estimation of multivariate location and scatter in the presence of cellwise and casewise contamination,” *Test*, 24, 441–461.
- Allison, K. H., Hammond, M. E. H., Dowsett, M., McKernin, S. E., Carey, L. A., Fitzgibbons, P. L., Hayes, D. F., Lakhani, S. R., Chavez-MacGregor, M., Perlmutter, J., Perou, C. M., Regan, M. M., Rimm, D. L., Symmans, W. F., Torlakovic, E. E., Varella, L., Viale, G., Weisberg, T. F., McShane, L. M., and Wolff, A. C. (2020), “Estrogen and Progesterone Receptor Testing in Breast Cancer: ASCO/CAP Guideline Update,” *Journal of Clinical Oncology*, 38, 1346–1366, PMID: 31928404.
- Atkinson, A. C., Riani, M., and Cerioli, A. (2010), “The forward search: theory and data analysis,” *Journal of the Korean Statistical Society*, 39, 117–134.

Table 3: Simulation results when  $(n, p) = (400, 40)$ . All measures are averaged over 50 random replicates. The numbers in parentheses are standard errors. Abbreviations are KL: Kullback–Leibler divergence, FDB: fast depth-based method algorithm, and Spec: spectral minimum covariance determinant.

Outlier	Metric	10%		25%		40%	
		FDB	Spec	FDB	Spec	FDB	Spec
Point	$e_\mu$	0.346	0.320	0.379	0.366	25.30	1.358
		(0.035)	(0.030)	(0.044)	(0.045)	(0.100)	(3.881)
	$e_\Sigma$	0.629	0.567	0.659	0.623	6.113	0.903
		(0.031)	(0.023)	(0.032)	(0.027)	(0.244)	(0.693)
	KL	2.870	2.375	3.148	2.826	231.1	18.54
		(0.163)	(0.096)	(0.191)	(0.153)	(2.744)	(58.79)
Cluster	$e_\mu$	0.351	0.328	0.369	0.355	0.405	0.400
		(0.037)	(0.034)	(0.035)	(0.037)	(0.040)	(0.038)
	$e_\Sigma$	0.624	0.566	0.658	0.619	0.722	0.712
		(0.032)	(0.026)	(0.036)	(0.025)	(0.029)	(0.027)
	KL	2.843	2.383	3.180	2.864	3.753	3.631
		(0.177)	(0.107)	(0.187)	(0.137)	(0.189)	(0.193)
Random	$e_\mu$	0.358	0.336	0.380	0.366	0.407	0.400
		(0.039)	(0.035)	(0.043)	(0.043)	(0.050)	(0.051)
	$e_\Sigma$	0.624	0.558	0.658	0.621	0.711	0.698
		(0.027)	(0.024)	(0.026)	(0.024)	(0.028)	(0.025)
	KL	2.853	2.358	3.177	2.878	3.732	3.597
		(0.169)	(0.108)	(0.155)	(0.134)	(0.175)	(0.155)
Radial	$e_\mu$	0.354	0.328	0.369	0.355	0.407	0.401
		(0.039)	(0.034)	(0.039)	(0.037)	(0.040)	(0.038)
	$e_\Sigma$	0.624	0.566	0.656	0.619	0.723	0.711
		(0.032)	(0.026)	(0.030)	(0.025)	(0.026)	(0.027)
	KL	2.837	2.383	3.184	2.864	3.748	3.632
		(0.174)	(0.107)	(0.187)	(0.137)	(0.189)	(0.193)

Table 4: Simulation results for  $(n, p) = (400, 80)$ . All measures are averaged over 50 random replicates. The numbers in parentheses are standard errors. Abbreviations are KL: Kullback–Leibler divergence, FDB: fast depth-based algorithm, and Spec: spectral minimum covariance determinant.

Outlier	Metric	10%		25%		40%	
		FDB	Spec	FDB	Spec	FDB	Spec
Point	$e_\mu$	0.575	0.469	0.605	0.522	35.52	3.057
		(0.049)	(0.037)	(0.048)	(0.045)	(1.320)	(7.715)
	$e_\Sigma$	1.125	0.855	1.161	0.956	7.122	1.555
		(0.039)	(0.027)	(0.038)	(0.028)	(0.334)	(1.424)
	KL	15.98	9.771	16.79	11.91	679.9	68.03
		(0.784)	(0.262)	(0.727)	(0.254)	(23.96)	(158.7)
Cluster	$e_\mu$	0.579	0.465	0.610	0.518	0.621	0.585
		(0.053)	(0.039)	(0.052)	(0.043)	(0.053)	(0.045)
	$e_\Sigma$	1.138	0.856	1.165	0.958	1.201	1.100
		(0.043)	(0.022)	(0.039)	(0.025)	(0.038)	(0.034)
	KL	16.22	9.776	16.75	11.97	17.70	15.39
		(0.760)	(0.248)	(0.716)	(0.304)	(0.574)	(0.389)
Random	$e_\mu$	0.582	0.467	0.601	0.519	0.607	0.572
		(0.053)	(0.037)	(0.051)	(0.036)	(0.052)	(0.052)
	$e_\Sigma$	1.143	0.862	1.173	0.952	1.215	1.109
		(0.037)	(0.022)	(0.044)	(0.028)	(0.038)	(0.038)
	KL	16.11	9.770	16.92	11.94	18.02	15.58
		(0.619)	(0.213)	(0.658)	(0.302)	(0.593)	(0.680)
Radial	$e_\mu$	0.586	0.465	0.594	0.518	0.627	0.585
		(0.054)	(0.039)	(0.054)	(0.043)	(0.050)	(0.045)
	$e_\Sigma$	1.143	0.856	1.167	0.958	1.215	1.110
		(0.043)	(0.022)	(0.05)	(0.025)	(0.043)	(0.034)
	KL	16.42	9.776	16.82	11.97	18.07	15.39
		(0.852)	(0.248)	(0.852)	(0.304)	(0.579)	(0.389)

Table 5: Simulation results for  $(n, p) = (2000, 200)$ . All measures are averaged over 50 random replicates. Abbreviations are KL: Kullback–Leibler divergence, FDB: fast depth-based method, and Spec: spectral minimum covariance determinant.

Outlier	Metric	10%		25%		40%	
		FDB	Spec	FDB	Spec	FDB	Spec
Point	$e_\mu$	0.369	0.338	0.389	0.365	56.30	9.748
		(0.015)	(0.009)	(0.014)	(0.016)	(1.944)	(19.71)
	$e_\Sigma$	0.663	0.589	0.706	0.650	6.932	1.613
		(0.008)	(0.006)	(0.010)	(0.010)	(0.375)	(1.836)
	KL	14.57	11.65	16.20	14.03	1157	265.2
		(0.258)	(0.156)	(0.225)	(0.132)	(21.15)	(522.0)
Cluster	$e_\mu$	0.372	0.337	0.388	0.360	0.414	0.406
		(0.017)	(0.014)	(0.019)	(0.018)	(0.017)	(0.016)
	$e_\Sigma$	0.665	0.589	0.703	0.649	0.756	0.734
		(0.011)	(0.008)	(0.011)	(0.011)	(0.007)	(0.007)
	KL	14.57	11.61	16.14	14.02	18.69	17.80
		(0.191)	(0.100)	(0.203)	(0.152)	(0.180)	(0.141)
Random	$e_\mu$	0.364	0.326	0.386	0.360	0.411	0.401
		(0.019)	(0.014)	(0.014)	(0.013)	(0.030)	(0.031)
	$e_\Sigma$	0.661	0.583	0.700	0.647	0.761	0.738
		(0.011)	(0.008)	(0.009)	(0.009)	(0.010)	(0.009)
	KL	14.54	11.61	17.79	16.12	18.67	17.73
		(0.247)	(0.054)	(0.527)	(0.217)	(0.277)	(0.329)
Radial	$e_\mu$	0.371	0.337	0.387	0.360	0.414	0.406
		(0.022)	(0.014)	(0.018)	(0.018)	(0.018)	(0.016)
	$e_\Sigma$	0.665	0.587	0.704	0.649	0.756	0.735
		(0.011)	(0.008)	(0.011)	(0.011)	(0.009)	(0.007)
	KL	14.58	11.61	16.22	11.97	18.83	17.80
		(0.247)	(0.010)	(0.199)	(0.304)	(0.185)	(0.141)

Table 6: Computation time averaged over 50 random replicates. Abbreviations are FDB: fast depth-based method, and Spec: spectral minimum covariance determinant.

Outlier	Combination	10%		25%		40%	
		FDB	Spec	FDB	Spec	FDB	Spec
Point	(400,40)	0.021	24.19	0.025	23.63	0.022	24.39
	(400,80)	0.092	31.40	0.062	27.79	0.074	31.70
	(2000,200)	2.382	574.1	2.478	607.3	2.391	605.7
Cluster	(400,40)	0.019	23.80	0.019	21.80	0.020	21.95
	(400,80)	0.066	32.60	0.064	29.47	0.073	31.35
	(2000,200)	2.029	521.7	2.128	559.6	1.981	513.6
Random	(400,40)	0.020	26.19	0.021	26.14	0.018	24.28
	(400,80)	0.086	72.74	0.081	59.13	0.069	56.38
	(2000,200)	2.301	1769	2.267	1680	1.929	1474
Radial	(400,40)	0.020	26.42	0.019	24.01	0.022	31.31
	(400,80)	0.068	55.57	0.083	58.18	0.070	57.00
	(2000,200)	2.194	1588	2.400	1751	2.059	1620

- Bauer, K. R., Brown, M., Cress, R. D., Parise, C. A., and Caggiano, V. (2007), “Descriptive analysis of estrogen receptor (ER)-negative, progesterone receptor (PR)-negative, and HER2-negative invasive breast cancer, the so-called triple-negative phenotype,” *Cancer*, 109, 1721–1728.
- Berenguer-Rico, V., Johansen, S., and Nielsen, B. (2023), “A model where the least trimmed squares estimator is maximum likelihood,” *Journal of the Royal Statistical Society Series B: Statistical Methodology*, 85, 886–912.
- Boudt, K., Rousseeuw, P. J., Vanduffel, S., and Verdonck, T. (2020), “The minimum regularized covariance determinant estimator,” *Statistics and Computing*, 30, 113–128.
- Butler, R., Davies, P., and Jhun, M. (1993), “Asymptotics for the minimum covariance determinant estimator,” *The Annals of Statistics*, 1385–1400.
- Cator, E. A. and Lopuhaä, H. P. (2012), “Central limit theorem and influence function for the MCD estimators at general multivariate distributions,” *Bernoulli*, 18, 520 – 551.
- Cerami, E., Gao, J., Dogrusoz, U., Gross, B. E., Sumer, S. O., Aksoy, B. A., Jacobsen, A., Byrne, C. J., Heuer, M. L., Larsson, E., Antipin, Y., Reva, B., Goldberg, A. P., Sander, C., and Schultz, N. (2012), “The cBio Cancer Genomics Portal: An Open Platform for Exploring Multidimensional Cancer Genomics Data,” *Cancer Discovery*, 2, 401–404.
- Ceroli, A. (2010), “Multivariate outlier detection with high-breakdown estimators,” *Journal of the American Statistical Association*, 105, 147–156.
- Fang, Y. and Wang, J. (2012), “Selection of the number of clusters via the bootstrap method,” *Computational Statistics & Data Analysis*, 56, 468–477.
- Filzmoser, P., Maronna, R., and Werner, M. (2008), “Outlier identification in high dimensions,” *Computational statistics & data analysis*, 52, 1694–1711.
- Grübel, R. (1988), “A minimal characterization of the covariance matrix,” *Metrika*, 35, 49–52.
- Hardin, J. and Rocke, D. M. (2005), “The distribution of robust distances,” *Journal of Computational and Graphical Statistics*, 14, 928–946.

- Haslbeck, J. M. and Wulff, D. U. (2020), “Estimating the number of clusters via a corrected clustering instability,” *Computational Statistics*, 35, 1879–1894.
- Hubert, M., Debruyne, M., and Rousseeuw, P. J. (2018), “Minimum covariance determinant and extensions,” *Wiley Interdisciplinary Reviews: Computational Statistics*, 10, e1421.
- Hubert, M., Rousseeuw, P. J., and Aelst, S. V. (2008), “High-Breakdown Robust Multivariate Methods,” *Statistical Science*, 23, 92 – 119.
- Hubert, M., Rousseeuw, P. J., and Vanden Branden, K. (2005), “ROBPCA: a new approach to robust principal component analysis,” *Technometrics*, 47, 64–79.
- Hubert, M., Rousseeuw, P. J., and Verdonck, T. (2012), “A deterministic algorithm for robust location and scatter,” *Journal of Computational and Graphical Statistics*, 21, 618–637.
- Hubert, M. and Van Driessen, K. (2004), “Fast and robust discriminant analysis,” *Computational Statistics & Data Analysis*, 45, 301–320.
- Lange, T., Mosler, K., and Mozharovskyi, P. (2014), “Fast nonparametric classification based on data depth,” *Statistical Papers*, 55, 49–69.
- Lemberge, P., De Raedt, I., Janssens, K. H., Wei, F., and Van Espen, P. J. (2000), “Quantitative analysis of 16–17th century archaeological glass vessels using PLS regression of EPXMA and  $\mu$ -XRF data,” *Journal of Chemometrics*, 14, 751–763.
- Li, C. and Jin, B. (2022), “Outlier Detection via a Block Diagonal Product Estimator,” *Journal of Systems Science and Complexity*, 35, 1929–1943.
- Li, C., Jin, B., and Wu, Y. (2024), “Outlier detection via a minimum ridge covariance determinant estimator,” *Statistica Sinica*, just-accepted.
- Meinshausen, N. and Bühlmann, P. (2010), “Stability selection,” *Journal of the Royal Statistical Society Series B: Statistical Methodology*, 72, 417–473.
- Network, T. C. G. A. (2012), “Comprehensive molecular portraits of human breast tumours,” *Nature*, 490, 61–70.

- Pokotylo, O., Mozharovskyi, P., and Dyckerhoff, R. (2016), “Depth and depth-based classification with R-package *ddalpha*,” *arXiv preprint arXiv:1608.04109*.
- Raymaekers, J. and Rousseeuw, P. J. (2023), “The cellwise minimum covariance determinant estimator,” *Journal of the American Statistical Association*, just-accepted.
- Riani, M., Atkinson, A. C., and Cerioli, A. (2009), “Finding an unknown number of multivariate outliers,” *Journal of the Royal Statistical Society Series B: Statistical Methodology*, 71, 447–466.
- Ro, K., Zou, C., Wang, Z., and Yin, G. (2015), “Outlier detection for high-dimensional data,” *Biometrika*, 102, 589–599.
- Rousseeuw, P. J. (1985), “Multivariate estimation with high breakdown point,” *Mathematical statistics and applications*, 8, 37.
- Rousseeuw, P. J. and Driessen, K. V. (1999), “A fast algorithm for the minimum covariance determinant estimator,” *Technometrics*, 41, 212–223.
- Rousseeuw, P. J. and Leroy, A. M. (2005), *Robust Regression and Outlier Detection*, John Wiley & Sons.
- Schreurs, J., Vranckx, I., Hubert, M., Suykens, J. A., and Rousseeuw, P. J. (2021), “Outlier detection in non-elliptical data by kernel MRCD,” *Statistics and Computing*, 31, 66.
- Sun, W., Wang, J., and Fang, Y. (2013), “Consistent selection of tuning parameters via variable selection stability,” *The Journal of Machine Learning Research*, 14, 3419–3440.
- Tibshirani, R., Walther, G., and Hastie, T. (2001), “Estimating the number of clusters in a data set via the gap statistic,” *Journal of the Royal Statistical Society: Series B (Statistical Methodology)*, 63, 411–423.
- Wang, J. (2010), “Consistent selection of the number of clusters via crossvalidation,” *Biometrika*, 97, 893–904.
- Wang, S., Nan, B., Rosset, S., and Zhu, J. (2011), “Random lasso,” *The annals of applied statistics*, 5, 468.



- Wen, C., Wang, Q., and Jiang, Y. (2023), “Stability Approach to Regularization Selection for Reduced-Rank Regression,” *Journal of Computational and Graphical Statistics*, 32, 974–984.
- Zhang, M., Song, Y., and Dai, W. (2023), “Fast robust location and scatter estimation: a depth-based method,” *Technometrics*, just-accepted.
- Zuo, Y. (2006), “Multidimensional trimming based on projection depth,” *The Annals of Statistics*, 34, 2211 – 2251.
- Zuo, Y. and Serfling, R. (2000a), “General notions of statistical depth function,” *The Annals of Statistics*, 461–482.
- (2000b), “Structural properties and convergence results for contours of sample statistical depth functions,” *The Annals of Statistics*, 483–499.